

---

# Investigation of the Nanocrystalline Formation with Activation Energy in $\text{Fe}_{72.5}\text{Ag}_2\text{Nb}_3\text{Si}_{13.5}\text{B}_9$ Metallic Ribbon Comparing with $\text{Fe}_{73.5}\text{Ag}_1\text{Nb}_3\text{Si}_{13.5}\text{B}_9$

Mohammad Mahmuduzzaman Tawhid<sup>1,\*</sup>, Rabiul Hassan<sup>1</sup>, Shibendra Shekher Sikder<sup>1</sup>,  
Mohammad Abdul Gafur<sup>2</sup>

<sup>1</sup>Department of Physics, Khulna University of Engineering and Technology, Khulna, Bangladesh

<sup>2</sup>Metallurgical Engineering Division, Bangladesh Council of Science & Industrial Research, Dhaka, Bangladesh

## Email address:

ku.tawhid@gmail.com (M. M. Tawhid)

\*Corresponding author

## To cite this article:

Mohammad Mahmuduzzaman Tawhid, Rabiul Hassan, Shibendra Shekher Sikder, Mohammad Abdul Gofur. Investigation of the Nanocrystalline Formation with Activation Energy in  $\text{Fe}_{72.5}\text{Ag}_2\text{Nb}_3\text{Si}_{13.5}\text{B}_9$  Metallic Ribbon Comparing with  $\text{Fe}_{73.5}\text{Ag}_1\text{Nb}_3\text{Si}_{13.5}\text{B}_9$ . *Engineering Physics*. Vol. 2, No. 2, 2018, pp. 41-47. doi: 10.11648/j.ep.20180202.12

**Received:** October 20, 2018; **Accepted:** November 1, 2018; **Published:** November 27, 2018

---

**Abstract:** This research focuses on the experimental investigation of nanocrystalline structure formation of  $\text{Fe}_{72.5}\text{Ag}_2\text{Nb}_3\text{Si}_{13.5}\text{B}_9$  alloys in the amorphous and annealed states. The sample like amorphous ribbon has been prepared by rapid solidification technique and their amorphous nature has been confirmed by X-ray diffraction (XRD). The crystallization behavior and the nanocrystal formation have been studied by Differential Thermal Analysis (DTA) and X-ray diffraction (XRD). The activation energy for crystallization is evaluated by Kissinger's plot. The ribbon sample has been annealed in a controlled way in the temperature range 550°C to 750°C for 2 hours. DTA runs for the sample show the existence of one exothermic peak for  $\alpha$ -Fe(Si) phase. Thermal analysis experiment and from the obtained data activation energy of primary crystallization products  $\alpha$ -Fe(Si) phase is 5.78 eV. After annealing the activation energy is found 0.164 eV. In the optimized annealing condition the grain size has been obtained in the range of 50 - 69nm. The peak shift indicates the change of the values of Si-content of nanograins. The activation energy is decreased after proper annealing at various temperatures. The crystallization phases of amorphous  $\text{Fe}_{72.5}\text{Ag}_2\text{Nb}_3\text{Si}_{13.5}\text{B}_9$  alloy annealed at temperature in the range of 550°C to 750°C for 2 hrs. is  $\alpha$ -Fe(Si) phases with average grain size 47 to 69 nm. These facts reveal that heat treatment temperature should be limited only 600°C at grain size 50nm to obtain optimum soft magnetic behavior, From XRD experiment, the crystallization onset temperature for the sample is around 600°C which coincides well with the value obtained DTA.

**Keywords:** Nanocrystals, DTA, XRD, Grain, Annealing

---

## 1. Introduction

It has been well established by the time through extensive research work that the addition of Cu and Nb, simultaneously with Fe-Si-B based amorphous alloys is the necessary condition for the extraordinary soft magnetic alloys called FINEMET having composition  $\text{Fe}_{73.5}\text{Nb}_3\text{Cu}_1\text{Si}_{13.5}\text{B}_9$ , developed in 1988 by Yoshizawa, Oguma and Yamauchi at Hitachi Metals Ltd. [1]. The Cu additives play a key role in the formation of the nucleation centers and Nb by inhibiting the grain growth [2]. This addition extends the temperature range between the primary crystallization of  $\alpha$ -Fe(Si) phase

and secondary crystallization  $\text{Fe}_2\text{B}$  phase for achieving superior magnetic properties [3]. It should be stressed again that good soft magnetic properties require not only a small grain size but at the same time the absence of boron compounds. Nanomaterials are generally materials that can have one dimension, two dimension or three dimension and can be specified within a size of 100 nanometer ( $1\text{nm}=10^{-9}\text{m}$ ). The separation between the primary crystallization of bcc  $\alpha$ -Fe and the precipitation of  $\text{Fe}_2\text{B}$  compounds is not only determined by Cu and Nb addition but also decrease with increasing content. This put a further constraint on the alloy composition namely that boron content should be kept at a

low or moderate level in order to obtain an optimum Nano scaled structure. Amorphous alloys provide an extremely convenient precursor material for preparation of nanocrystals through the crystallization process controlled by thermal treatments [4 -7]. Müller *et al.* [8] studied the influence of Cu/ Nb content and annealing condition on the microstructure and the magnetic properties of FINEMET alloys. Grain size, phase composition and transition temperature were observed to depend on the Cu/Nb content. Investigations have been carried out on the effect of substitution of Au for Cu in the FINEMET on the crystallization behavior [9]. Magnetic materials played a prominent role in the discovery of new civilization and development of modern technology. Over the past several decades, amorphous and most recently, research interest in nanocrystalline soft magnetic alloys has dramatically increased. Soft magnetic materials face demanding requirements for high performance electronic and power distribution systems. With the reduction of size into nanometer range, the materials exhibit interesting properties including physical, chemical, magnetic and electrical properties comparing to conventional coarse grained counterparts. Soft magnetic Nano structured materials have a number of potential technological applications.[10-16] DTA of cast sample, annealing, XRD and again DTA these experiments were done one by one to find the crystalline formation state and activation energy.

## 2. Materials and Methods

The amorphous ribbon with a composition  $Fe_{72.5}Ag_2Nb_3Si_{13.5}B_9$  was prepared from high purity Fe (99.9%), Ag (99.9%), Nb (99.9%), Si (99.9%) and B (99.9%). The ribbons were produced in an arc furnace on a water-cooled copper hearth by a single roller melt-spinning technique under an atmosphere of pure argon at the Centre of Materials Science, National University of Hanoi, Vietnam. The wheel velocity was about 34 m/s. The ribbons were annealed in a vacuum heat treatment furnace at 625, 700, 725 and 750°C respectively for constant time 30 minutes and then

cooled down to the room temperature. Crystallization phase analysis was carried out by DTA. The activation energy for crystallization of primary and secondary phases have been calculated using Kissinger's equation [14]:  $E = -kT_p \ln\left(\frac{\beta}{T_p^2}\right)$ , where  $\beta$  is the heating rate,  $T_p$  is the crystallization peak temperature,  $E$  is the activation energy and  $k$  is the Boltzman's constant. Amorphousness of the ribbon and nanocrystalline structure have been observed by XRD (Philips (PW 3040) X 'Pert PRO XRD) with Cu-K $\alpha$  radiation. Grain size ( $D_g$ ) of all annealed samples of the alloy composition has been determined using Sherrer method.

## 3. Results and Discussion

### 3.1. DTA

It is clear from Figure-1(a) to 1(f) that one exothermic peak is found for the sample  $Fe_{72.5}Ag_2Nb_3Si_{13.5}B_9$ . The peak temperature,  $T_p$  displays exothermic peak, i.e., release of heat during the crystallization of  $\alpha$ -Fe-(Si) phase. DTA traces of as-cast amorphous ribbons  $Fe_{72.5}Ag_2Nb_3Si_{13.5}B_9$  with heating at the rate of 10–60°C/min at the step of 10°C with continuous heating from room temperature to 900°C are shown in the figure-1. It is observed that the crystallization of the phase has occurred over a wide range of temperatures.

It is also observed that the peak temperature shifted towards the higher value and the crystallization temperature range increases with the increase of heating rate. That means, it requires more heat energy for the formation of crystalline phase with increasing heating rate. The heat consumption is observed during the primary crystallization. The peak is shifting in the range from 569°C -600°C is evident from the figure 1.

From the Figure-2(a) and Figure-2(b) the activation energy for the  $\alpha$ -Fe-(Si) phase is found to be  $E = 5.78$  eV and  $E = 0.164$  eV for before and after annealing respectively. The values of crystallization onset temperature, peak temperature with respect to heating rate and activation energy are listed in the Table 1.

**Table 1.** The values of crystallization onset temperature, peak temperature with respect to heating rate and activation energy of the nanocrystalline amorphous ribbon with composition  $Fe_{72.5}Ag_2Nb_3Si_{13.5}B_9$ .

Heating rate $\beta$ °C/min	1 <sup>st</sup> starting $T_{x1}$ °C (Onset temperature)	1 <sup>st</sup> Peak $T_{p1}$ °C (Peak temperature)	Temperature range of 1 <sup>st</sup> state in °C	Activation Energy of the peak before annealing	Activation Energy of the peak after annealing
10	569.69	579	9.31	5.78 eV	0.164 eV
20	575.69	592.49	16.8		
30	571.02	598.68	27.66		
40	581.10	595.11	14.01		
50	586.64	600.68	14.04		
60	590.67	607.78	17.11		

“ $\beta$  = Heating rate,  $T_{x1}$  = Onset temperature,  $T_{p1}$  = Peak temperature, eV = Electron Volt =  $-1.6 \times 10^{-19}$  Coulomb”

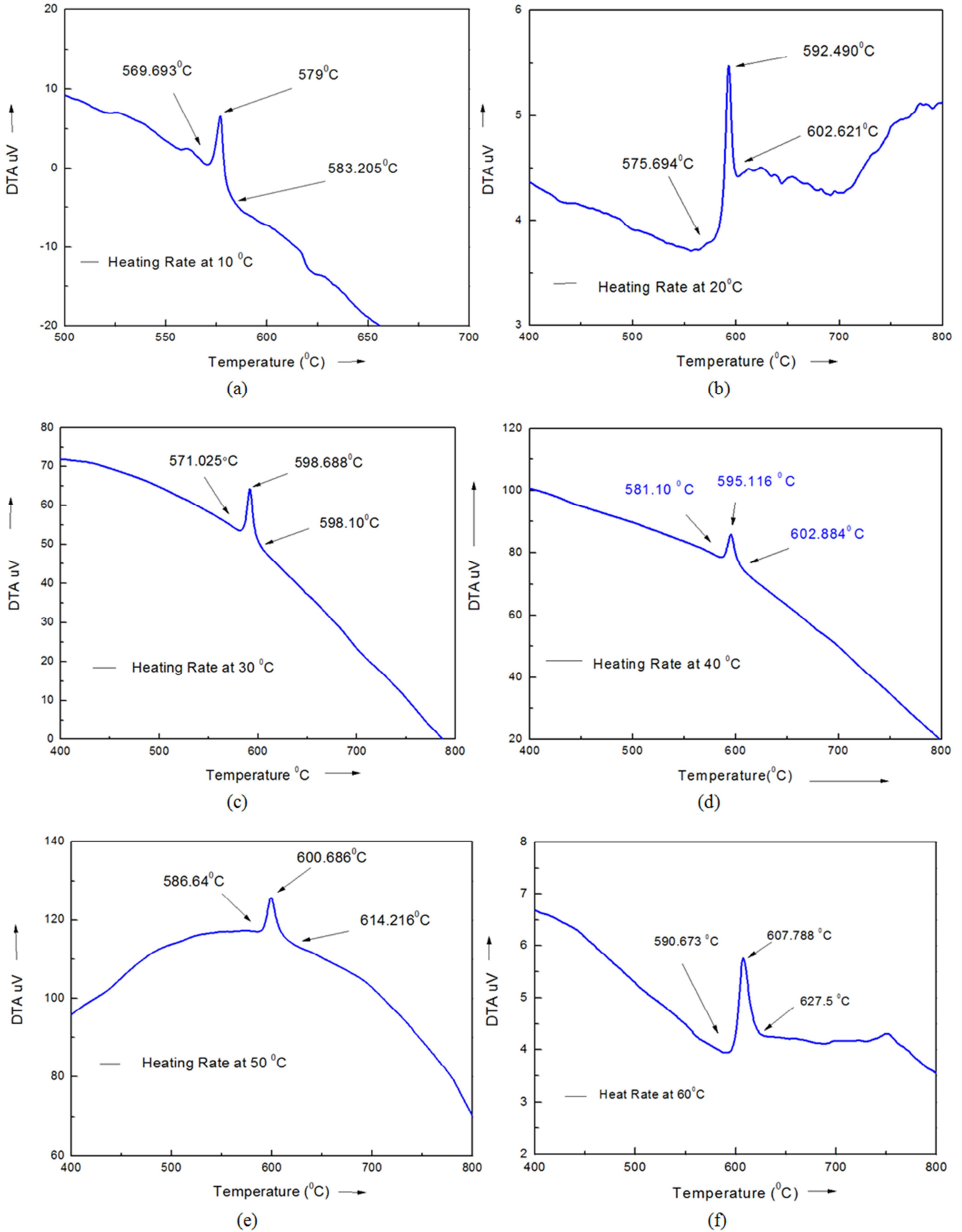


**Figure 1.** DTA trace of as cast amorphous ribbon  $Fe_{72.5}Ag_2Nb_3Si_{13.5}B_9$  ribbon at the heating rate of (a) 10°C/min (b) 20°C/min (c) 30°C/min (d) 40°C/min (e) 50°C/min (f) 60°C/min.

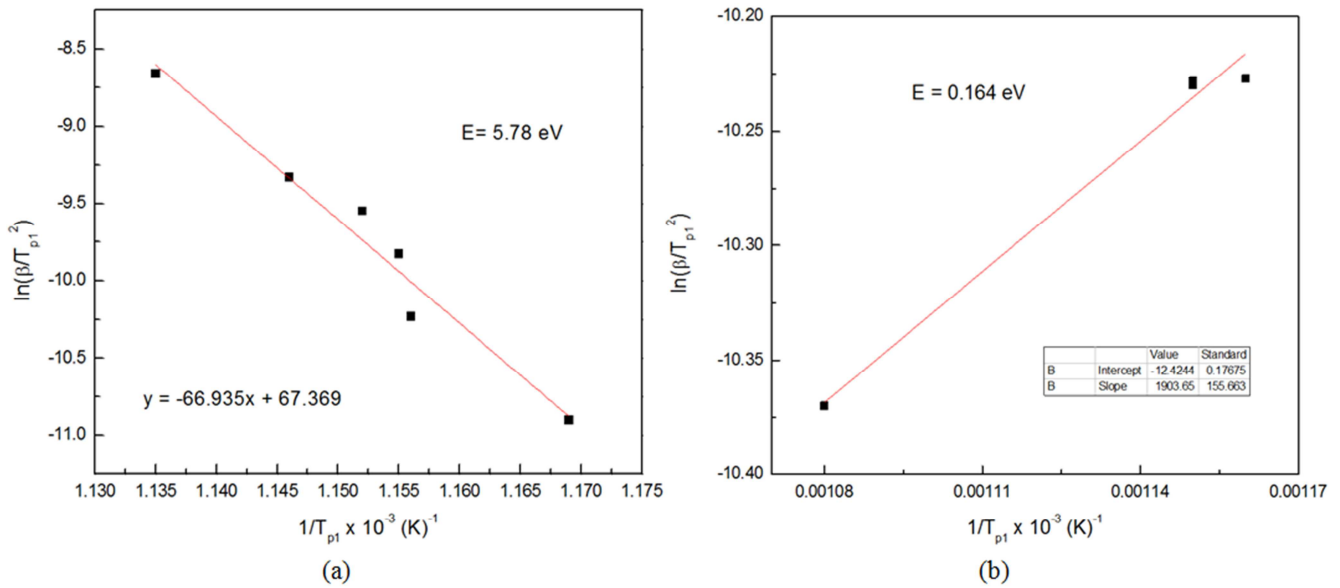


Figure 2. Kissinger's plot to determine the activation energy of  $\alpha$ -Fe(Si) phase for (a) before annealing (b) after annealing.

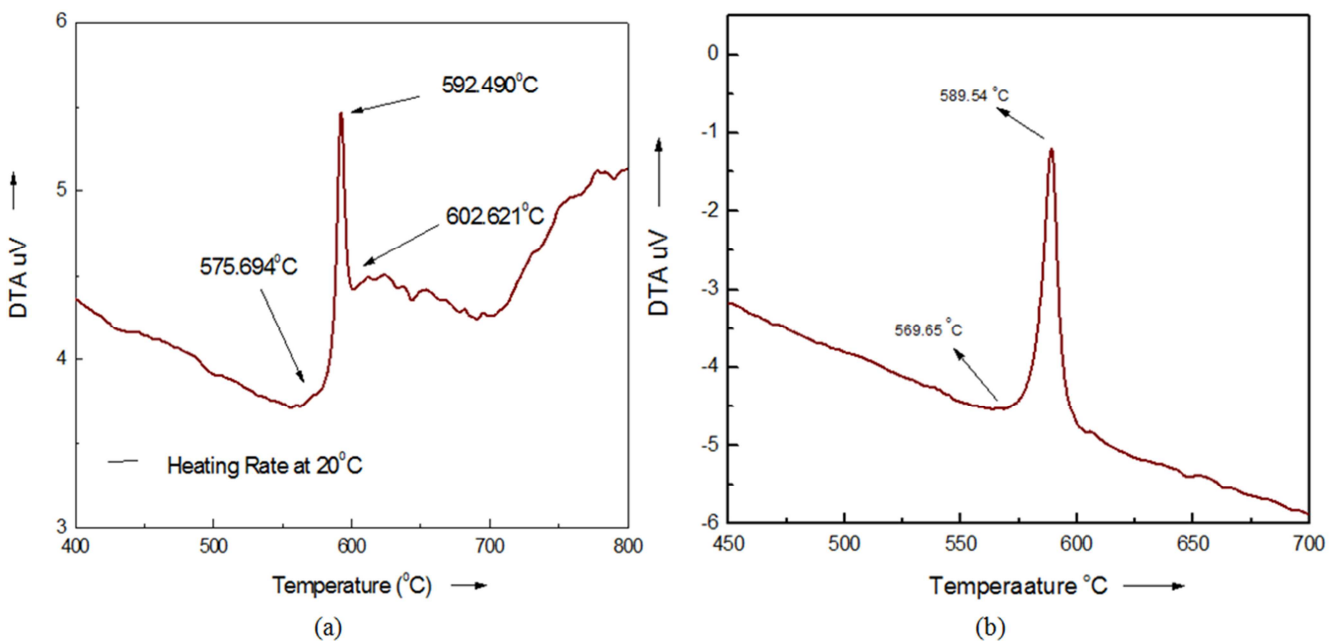
### 3.2. Annealing

The experimental data have been interpreted in terms of different annealing effects on amorphous ribbons of DTA traces at constant heating rate 20°C/min. The DTA traces of Fe<sub>72.5</sub>Ag<sub>2</sub>Nb<sub>3</sub>Si<sub>13.5</sub>B<sub>9</sub> alloy in the as cast state and annealed at different temperatures for 2 hrs. are shown in Figure 3(a) to 3(d), respectively. It is observed from the DTA scan that the onset temperature for the sample Fe<sub>72.5</sub>Ag<sub>2</sub>Nb<sub>3</sub>Si<sub>13.5</sub>B<sub>9</sub> annealed at T = 550°C is almost unchanged with respect to its amorphous precursor which is quite logical since T = 550°C is still lower than its  $T_{x1} = 579^\circ\text{C}$ . But the same sample when annealed at  $T_a = 600^\circ\text{C}$  and  $650^\circ\text{C}$  which are higher than the

onset of crystallization temperature of  $T_{x1} = 579^\circ\text{C}$ , the primary crystallization peak is becoming smaller and display diffused character meaning that substantial amount of primary crystallization,  $\alpha - Fe(Si)$  phase has already been completed for 2 hours at  $T_a = 600^\circ\text{C}$  and  $T_a = 650^\circ\text{C}$ .

### 3.3. Comparison

Comparison of effect of heating rate on 1<sup>st</sup> and 2<sup>nd</sup> crystallization states and activation energy of Fe<sub>73.5</sub>Cu<sub>1</sub>Nb<sub>3</sub>Si<sub>13.5</sub>B<sub>9</sub>, Fe<sub>73.5</sub>Ag<sub>1</sub>Nb<sub>3</sub>Si<sub>13.5</sub>B<sub>9</sub>, Fe<sub>72.5</sub>Ag<sub>2</sub>Nb<sub>3</sub>Si<sub>13.5</sub>B<sub>9</sub> are mentioned below.



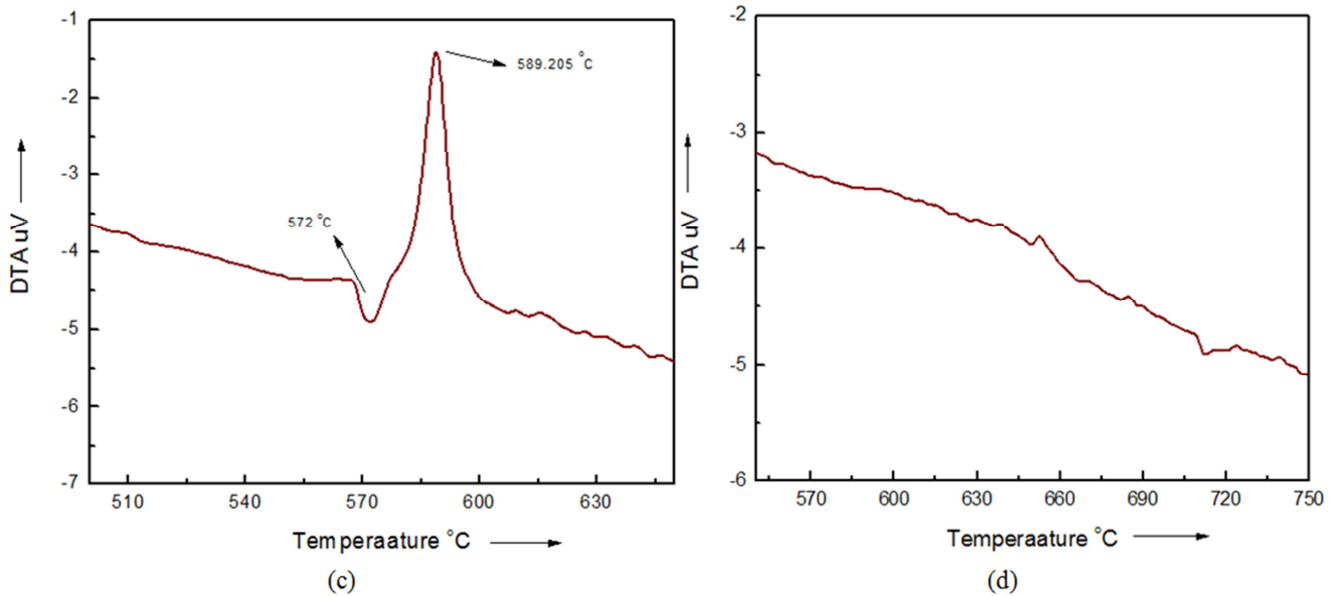


**Figure 3.** Effects on DTA trace of annealing temperature on the nanocrystalline amorphous ribbon with composition  $Fe_{72.5}Ag_2Nb_3Si_{13.5}B_9$  at the heating rate of  $20^\circ C/min$  (a) as cast (b) at  $550^\circ C$  (c) at  $600^\circ C$  (d) at  $650^\circ C$ .

**Table 2.** Comparison of effect of heating rate on 1<sup>st</sup> and 2<sup>nd</sup> crystallization states and activation energy of various nanocrystalline amorphous ribbons.

Sample	Heating Rate in $^\circ C/min$	$T_{p1}$ in $^\circ C$	$T_{p2}$ in $^\circ C$	$E_1$ in eV	$E_2$ in eV
$Fe_{73.5}Cu_1Nb_3Si_{13.5}B_9$ [17]	10-50	542-570	868-719	3.21	3.81
$Fe_{73.5}Ag_1Nb_3Si_{13.5}B_9$ [18]	10-50	590-614	767-785	4.37	4.45
$Fe_{72.5}Ag_2Nb_3Si_{13.5}B_9$	10-60	579-608	-----	5.78	-----

" $T_{p1}$  = First Peak temperature,  $T_{p2}$  = Second Peak temperature,  $E_1$  = First Peak Activation Energy,  $E_2$  = Second Peak Activation Energy, eV = Electron Volt =  $-1.6 \times 10^{-19}$  Coulomb"

### 3.4. XRD

After annealing the sample from  $550^\circ C$  to  $750^\circ C$  we found XRD spectra which has been presented by figure-3. In the case of as cast state, there has a broadened peak which could be the evidence of noncrystalline amorphous. It is evident from Figure-3 when the sample annealed at  $550^\circ C$ , it exhibited small peak around  $2\theta = 45^\circ$  angle at the position of  $d_{110}$  reflection which is generally known as diffuse hallow. This diffuse hallow indicates the amorphous nature of the sample. It means at this temperature, no crystallization peak has been detected. So the onset crystallization temperature determined from these results is  $550^\circ C$ .

In the case of as cast state, there has a broadened peak which could be the evidence of noncrystalline amorphous. It is evident from Figure-4 when the sample annealed at  $550^\circ C$ , it exhibited small peak around  $2\theta = 45^\circ$  angle at the position of  $d_{110}$  reflection which is generally known as diffuse hallow. This diffuse hallow indicates the amorphous nature of the sample. It means at this temperature, no crystallization peak has been detected. With the increasing of Annealing temperature  $T_a$ , (110) peak becomes sharper which means the grains are growing bigger. Absence of boride phase in the XRD spectra is possibly due to very small volume fraction of  $Fe_{23}B_6$ . The value of full width half maxima (FWHM) of the peak at the annealing temperature  $550^\circ C$  was not detected due to the lack of sharp peak. For the higher annealing

temperatures, the FWHM value is getting smaller. It shows that the crystallization occurs to a good extent at the higher annealing temperature. The crystallization onset temperatures from DTA experiment for different heating rates were found in the range of  $579^\circ C$ , which shows a good consistency with the XRD results. The lattice parameter, the silicon content in bcc nanograins and grain size of  $\alpha$ -Fe(Si) grain can easily be calculated from the fundamental peak of (110) reflections. All results are shown in Table 3.

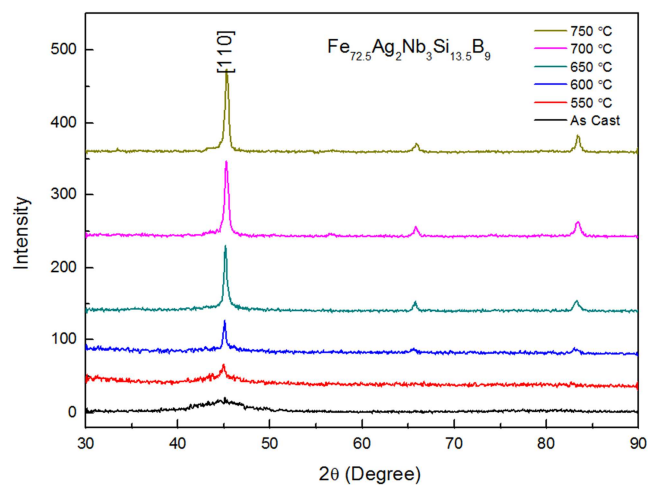


**Figure 4.** XRD spectra of  $Fe_{72.5}Ag_2Nb_3Si_{13.5}B_9$  alloys of as cast and annealed at different temperatures at constant annealing time 2 hours.

**Table 3.** Experimental XRD data of nanocrystalline  $Fe_{72.5}Ag_2Nb_3Si_{13.5}B_9$  amorphous ribbon at different annealing temperatures.

Annealing Temp. in °C	$\theta$ (deg.)	d (Å)	$\beta$ FWHM (deg.)	$a_0$ (Å)	$D_g$ (nm)	Si (at. %)
As Cast	22.61	2.0028	.....	1.4161	.....	6.660
550	22.50	2.0121	.....	1.4227	.....	6.629
600	22.57	2.0061	0.3010	1.4185	50	6.648
650	22.57	2.0061	0.2178	1.4185	69	6.648
700	22.61	2.0028	0.2614	1.4162	58	6.659
750	22.65	1.9994	0.2179	1.4137	69	6.670

“ $\beta$  = Full Width Half Maxima (FWHM),  $\theta$  = Angle, d = Width of the peak,  $a_0$  = Lattice Parameter,  $D_g$  = Grain Size, Si (at. %) = Silicon Content in percentage”

Grain size is determined by this equation:  $D_g = \frac{0.9\lambda}{\beta \cos \theta}$

Comparison of experimental XRD data of grain size at different annealing temperatures of various nanocrystalline ribbons is presented below:

**Table 4.** Comparison of experimental XRD data of grain size at different annealing temperatures of nanocrystalline ribbons.

Annealing Temperature in °C	Grain size of $Fe_{73.5}Cu_1Nb_3Si_{13.5}B_9$ [10], $D_g$ (nm)	Grain size of $Fe_{73.5}Ag_1Nb_3Si_{13.5}B_9$ [11], $D_g$ (nm)	Grain size of $Fe_{73.5}Ag_2Nb_3Si_{13.5}B_9$ , $D_g$ (nm)
550	10	-----	-----
575	11	-----	-----
600	11	-----	50
650	11	10	69
675	14	-----	-----
700	22	9	58
750	-----	20	69
800	-----	30	-----

“ $D_g$  = Grain Size, nm = Nano meter (1 Nano meter =  $10^{-9}$  meter)”

## 4. Conclusion

DTA experiments were performed for six different heating rates 10 to 60°C/min. in steps of 10°C/min. up to a temperature of 800°C. DTA reveals, one exothermic peak is distinctly observed which corresponds to crystallization event temperature  $T_{x1}$  [ $\alpha$ -Fe(Si)] indicates stability of amorphous state of structural stability and magnetic ordering values of 579°C for  $Fe_{72.5}Ag_2Nb_3Si_{13.5}B_9$  with heating rate 20°C/min.

The activation energy of the first crystallization phase  $\alpha$ -Fe(Si) calculated using Kissinger’s plot. Activation energy of  $\alpha$ -Fe(Si) phase is 5.78eV.

The amorphous stage of the as- cast ribbon has been confirmed by XRD. The evolution of the primary phase on annealed samples has been confirmed as  $\alpha$ -Fe(Si) and their sizes have been determined from the line broadening of fundamental peaks (110) from XRD pattern as affected by annealing around the crystallization temperature. The crystallization phases of amorphous  $Fe_{72.5}Ag_2Nb_3Si_{13.5}B_9$  alloy annealed at temperature in the range of 550°C to 750°C for 2 hrs. is  $\alpha$ -Fe(Si) phases with average grain size 47 to 69 nm. These facts reveal that heat treatment temperature should be limited only 600°C at grain size 50nm to obtain optimum soft magnetic behavior, From XRD experiment, the crystallization onset temperature for the sample is around 600°C which coincides well with the value obtained DTA.

## References

- [1] Yoshizawa Y., Oguma S. and Yamauchi K.; “New Fe-based soft magnetic alloys composed of ultra fine grain structure”; J. Appl. Phys. 64, 6044 – 6046, 1988.
- [2] Jing Zhi, Kai-Yuan He, Li-Zhi Cheng and Yu-Jan Fu; “Influence of the elements Si/B on the structure and magnetic properties of Nanocrystalline  $(FeCuNb)_{77.5}Si_xB_{22.5-x}$  Alloys”; J. Magn. Magn. Mater., 153, 315, 1996.
- [3] Herzer G; “Nanocrystalline Soft Magnetic Alloys”; in Hand Book of Materials, Vol. 10 ed; K. H. J. Buchow, Elsevier Pub. Co., 1997.
- [4] Herzer G; “Grain structure and Magnetism of Nanocrystalline Ferromagnetic”; IEEE Trans. Magn., 26, 1397 - 1402., 1990.
- [5] Hakim M. A. and Hoque S. M.; “Effect of Structural Parameters on Soft Magnetic properties of two phase nanocrystalline alloy of  $Fe_{73.5}Cu_1Ta_3Si_{13.5}B_9$ ”; J. Magn. Magn. Mater., 284, 395 - 402, 2004.
- [6] Sarout Noor, Sikder S. S., Saha D. K. and Hakim M. A.; “Time and Temperature Dependence of Nanocrystalline and Initial Permeability of Finement alloys”; Nuclear Science and Application; 15, 1, 9 - 13, 2016.
- [7] Mondal S. P., Kazi Haniun Maria, Sikder S. S., Shamima Chowdhury, Saha D. K. and Hakim M. A.; “Influence of Annealing Conditions in Nanocrystalline and Ultra soft Magnetic properties of  $Fe_{73.5}Cu_1Nb_3Si_{13.5}B_9$ ”; J. Mater. Sci Technol., 28 (1), 21 - 26, 2012.

- [8] Müller M., Matterm N. and Kuhn U.; “Corelation between magnetic and structural properties of Nanocrystalline soft magnetic alloys”; *J. Magn. Mater.*, 157/158, 209 - 210, 1996.
- [9] Saha D. K. and Hakim M. A.; “Crystallization Behaviour of  $\text{Fe}_{73.5}\text{Au}_1\text{Nb}_3\text{Si}_{13.5}\text{B}_9$ ”; *Bang. J. Acad. Sci.*, 30, No. 2, 177 - 187, 2006.
- [10] Jie Chen, Zhenghou Zhu, “The study on surface chemical modification of  $\text{Fe}_{71.5}\text{Cu}_1\text{Nb}_3\text{Si}_{13.5}\text{B}_9\text{V}_2$  amorphous alloy ribbons and its piezomagnetic effect”, *J. Magn. Magn. Mater.* (2016) 419, 451-455.
- [11] C. Miguel, A. P. Zhuov, J. Gonzalez, “Magnetoimpedance of stress and/ or field annealed  $\text{Fe}_{73.5}\text{Cu}_1\text{Nb}_3\text{Si}_{15.5}\text{B}_7$  amorphous and nanocrystalline ribbon”, *J. Magn. Magn. Mater.* (2003) 254-255, 463-465.
- [12] Trilochan Sahoo, B. Mojumdar, V. Srinivas, M. Srinivas, T. K. Nath, G. Agarwal, “Improved magnetoimpedance and mechanical properties on nanocrystallization of amorphous  $\text{Fe}_{68.5}\text{Si}_{18.5}\text{Cu}_1\text{Nb}_3\text{B}_9$  ribbons”, *J. Magn. Magn. Mater.* (2013) 343, 13-20.
- [13] Partha Sarkar, O. Mohanta, S. K. Pal, A. K. Panda, A. Mitra, “Magneto-Impedance behavior of Co-Fe-Nb-Si-B based ribbons”, *J. Magn. Magn. Mater.* (2010) 322 (8), 1026-1031.
- [14] S. N. Kane, S. Sarabhi, A. Gupta, L. K. Varga, T. Kulik, “Effect of quenching rate on crystallization in  $\text{Fe}_{73.5}\text{Si}_{13.5}\text{B}_9\text{Cu}_1\text{Nb}_3$  alloy”, *J. Magn. Magn. Mater.* (2000) 215-216, 372.
- [15] S. P. Mondal, Kazi Haniun Maria, S. S. Sikder, Shamima Choudhury, D. K. Saha, M. A. Hakim, “Influence of Annealing Conditions on Nanocrystalline and Ultra-Soft Magnetic Properties of  $\text{Fe}_{73.5}\text{Cu}_1\text{Nb}_3\text{Si}_{13.5}\text{B}_9$  alloy”, *J. Mater. Sci. Technol.*, 2012, 28 (1), 21-26.
- [16] M. Hassiak, J. Zbrozarczyk, J. Olszewki, W. H. Ciuzynska, B. Wyslocki, A. Blachowicz, “Effect of cooling rate on magnetic properties of amorphous and nanocrystalline  $\text{Fe}_{73.5}\text{Cu}_1\text{Nb}_3\text{Si}_{13.5}\text{B}_9$  alloy”, *J. Magn. Magn. Mater.* (2000) 215-216, 410.
- [17] Sarout Noor; M. Phil. Thesis, KUET, p. 99, March 2005.
- [18] Asaduzzaman A. K. M.; M. Phil. Thesis, KUET, p. 86, December 2016.